

Evidence of low-dimensional antiferromagnetic ordering and crystal structure in the $R_2\text{BaNiO}_5$ ($R = \text{Y, Er}$) oxides

J. Amador, E. Gutiérrez-Puebla,* M. A. Monge,* I. Rasines,[†] and C. Ruíz-Valero*
*Instituto de Ciencia de Materiales, Consejo Superior de Investigaciones Científicas,
 Serrano 113, 28006 Madrid, Spain*

F. Fernández and R. Sáez-Puche
*Departamento de Química Inorgánica, Facultad de Ciencias Químicas, Universidad Complutense,
 28040 Madrid, Spain*

J. A. Campá
*Departamento de Cristalografía y Mineralogía, Facultad de Ciencias Geológicas,
 Universidad Complutense, 28040 Madrid, Spain*

(Received 28 December 1989; revised manuscript received 12 June 1990)

Crystals of $R_2\text{BaNiO}_5$ ($R = \text{Y, Er}$) have been grown, and their structures have been established by single-crystal x-ray diffraction. Both compounds crystallize in the $\text{Nd}_2\text{BaNiO}_5$ structure type, with one-dimensional chains of vertex-sharing NiO_6 octahedra in the direction of the a axis. These octahedra show an unusual twofold distortion: The Ni-O distances to the two axial oxygen atoms are considerably shorter, 0.3 Å, than those to the four equatorial oxygens, and these oxygens are distorted from the right angles of a regular octahedron to $79.0(2)^\circ$ or $77.7(6)^\circ$, respectively. As a result of this, Ni-O(axial)-Ni distances are very short, 3.76 and 3.75 Å for $R = \text{Y}$ and Er , respectively. X-ray powder diffraction data and the results of magnetic measurements for both oxides are given. The structural features mentioned elucidate why Ni^{2+} ions in polycrystalline Y_2BaNiO_5 behave as a monodimensional system in which they become antiferromagnetically ordered below 300 K. Besides that, the ferromagnetic interactions that operate below 40 K can be due to tridimensional interchain interactions and/or the presence of ferromagnetic impurities. The estimated Néel temperature for Y_2BaNiO_5 , higher than that reported for Y_2BaCuO_5 , is explained by the promotion of the superexchange Ni-O-Ni interactions along the chains of flattened NiO_6 octahedra sharing corners. In $\text{Er}_2\text{BaNiO}_5$ both effects are masked by the strong paramagnetic signal of Er^{3+} , and a maximum observed at 15.6 K for the susceptibility is attributed to tridimensional ordering of the Er^{3+} cations.

INTRODUCTION

Polycrystalline samples of a new family of oxides of general formula $R_2\text{BaMO}_5$, where R stands for a trivalent rare-earth cation and M represents Cu or Zn, were first prepared and characterized by the group of Raveau^{1,2} in the early 1980s. The Cu compounds with R from Sm to Tm are isostructural,¹ space group (SG) $Pnma$, and have a framework built up through edge and face sharing of RO_7 monocapped trigonal prisms, with the M atoms showing a pyramidal MO_5 coordination, which has been established^{3,4} in single crystals of two compounds. The $R_2\text{BaCuO}_5$ oxides, which appear sometimes as impurities of the new high-temperature superconductors of the composition $R\text{Ba}_2\text{Cu}_3\text{O}_{7-x}$, have been designed as the *green phases*, while the isostoichiometric Zn compounds, being light colored, have been studied from the point of view of their optical properties.⁵ As for Y_2BaCuO_5 , magnetic measurements and neutron diffraction studies have shown⁶ that copper moments order antiferromagnetically in this oxide at about 28 K.

The first example of a new family of oxides formulated as $R_2\text{BaNiO}_5$ ($R = \text{Nd}$) was described by Müller-

Buschbaum and co-workers⁷ in the SG $Immm$. Unlike tetragonal pyramidal Cu or Zn in $R_2\text{BaMO}_5$, Ni in $\text{Nd}_2\text{BaNiO}_5$ forms chains of flattened NiO_6 octahedra with four oxygens at a larger distance than the other two. Subsequent studies established⁸⁻¹⁰ the same crystal structure for the majority of the compounds with R from Sm to Tm. Independently, our group prepared and characterized¹¹ polycrystalline samples of nine $R_2\text{BaNiO}_5$ oxides ($R = \text{Y, Nd, Sm, Eu, Gd, Dy, Ho, Er, or Tm}$) and, after growing single crystals, determined¹² the structure of the Gd compound following an anisotropic refinement which led to a discrepancy factor of 0.019 and to the following Ni-O internuclear distances: 4 of 2.197(6) Å and 2 of 1.8936(2) Å. This unusual distortion away from the ordinary octahedral coordination about Ni, as well as the existence of one-dimensional (1D) chains of vertex-sharing octahedra in the direction of the a axis with extremely short Ni-O-Ni distances (3.79 Å in the Gd compound¹²), suggested interesting physical properties.

On the other hand, nearest oxygens to Ni are distorted from the 90° angles of a regular octahedron to $79.6(2)^\circ$. These observations¹² have been recently shown¹³ understandable using a model which combines results from

molecular-orbital theory, tight-binding band-structure calculations, and empirical atom-atom potential arguments. In order to apply this combination of methods, x-ray diffraction data are needed from anisotropic refinements as good as possible. In addition, the possibility of obtaining nonstoichiometric samples of these oxides cannot be conclusively discarded: For example, in the case of the Cu compounds, it seems that nonstoichiometric crystals have been obtained.⁴ In these cases precise x-ray diffraction data are also needed for determining the population factors of the oxygen atoms. In the present paper we report the interesting magnetic properties of two of these oxides, $R_2\text{BaNiO}_5$ ($R = \text{Y, Er}$), as well as their crystal structures and x-ray diffraction data. As far as we know, one of them, $R = \text{Y}$, has been prepared for the first time. Although the crystal structure of the Er compound is known,⁸ it was determined through an isotropic refinement which led to a high discrepancy factor, 0.103.

EXPERIMENTAL ASPECTS

Tiny prismatic crystals, black colored, of composition $R_2\text{BaNiO}_6$ ($R = \text{Y, Er}$) were grown after adding $R_2\text{O}_3$ to a mixture of an excess of Ni metal with $\text{Ba}(\text{OH})_2 \cdot 8\text{H}_2\text{O}$ held at 100 °C, heating to 1150 °C, and quenching in air. $\text{Er}_2\text{BaNiO}_5$ crystals were polysynthetically twinned. The crystals were mounted in a Kappa diffractometer. A summary of the fundamental crystal and refinement data is given in Table I. The cell dimensions were refined by least-squares fitting the 2θ values of 25 reflections. The

intensities were corrected for Lorentz and polarization effects. Scattering factors for neutral atoms and anomalous dispersion corrections for Y, Er, Ba, and Ni were taken from the International Tables for X-ray Crystallography.¹⁴ The structure was solved by Patterson and Fourier methods. An empirical absorption correction was applied at the end of the isotropic refinement.¹⁵ After anisotropic full-matrix least-squares refinement, a final difference synthesis had no significant electron density. Most of the calculations were carried out with the X-ray 80 System.¹⁶ Polycrystalline $R_2\text{BaNiO}_5$ ($R = \text{Y, Er}$) samples for magnetic measurements were prepared from stoichiometric mixtures of analytical grade $R_2\text{O}_3$, BaO_2 , and NiO , that were ground, pelletized, and heated in air for 12 h at 900, 1000, 1100, and 1200 °C. After each thermal treatment, the products were quenched, reground, and pelletized. The x-ray diffraction data for polycrystalline samples were measured and calculated as indicated elsewhere.¹⁷ For the calculation of the intensities of polycrystalline $R_2\text{BaNiO}_5$ ($R = \text{Y, Er}$) the atomic positions and temperature factors obtained after solving the crystal structures were employed. Magnetic susceptibility measurements were made in the 4.2–300 K temperature range as pointed out elsewhere.¹⁷ The susceptibility, χ , was independent of the field at all temperatures for $\text{Er}_2\text{BaNiO}_5$, while in the case of the Y compound a small susceptibility dependence with the temperature below 40 K was observed. The molar susceptibilities were corrected for ionic diamagnetism using the values,¹⁸ in 10^{-6} emu mol⁻¹, of -12 for O^{2-} , Ni^{2+} and Y^{3+} ; -18 for Er^{3+} ; and -32 for Ba^{2+} .

TABLE I. Crystal and refinement data for $R_2\text{BaNiO}_5$ ($R = \text{Er, Y}$).

Formula	$\text{BaEr}_2\text{NiO}_5$	BaY_2NiO_5
Crystal system	Orthorhombic	Orthorhombic
Space group ^a	<i>Immm</i>	<i>Immm</i>
a (Å)	3.747(2)	3.7610(6)
b (Å)	5.737(2)	5.7610(7)
c (Å)	11.283(2)	11.323(2)
V (Å ³)	242.5(2)	245.34(7)
Z	2	2
$F(000)$	520	404
ρ (calc) (g cm ⁻³)	8.36	6.14
t (°C)	21	21
μ (cm ⁻¹)	465.2	352.3
Cryst. dimens. (mm ³)	0.1 × 0.1 × 0.25	0.04 × 0.04 × 0.2
Diffractometer	Enraf-Nonius CAD4	Enraf-Nonius CAD4
Radiation	Graphite-monochromated Mo $K\alpha$ ($\lambda = 0.71069$ Å)	Graphite-monochromated Mo $K\alpha$ ($\lambda = 0.71069$ Å)
Scan technique	$\Omega/2\theta$	$\Omega/2\theta$
Data collected	(0,0,0) to (5,8,16)	(0,0,0) to (5,8,16)
Unique data	250	254
Unique data ($I \geq 2\sigma(I)$)	249	228
Std. rflns.	3 rflns.	3 rflns.
Decay	$\leq 1\%$ variation	
R_F^b (%)	4.4	2.3
Average shift/error	0.006	0.002
Maximum shift/error	0.03	0.01

^aReference 14, Vol. IV, pp. 314–315.

^b $R_F = \sum_{\text{ref}} (|F_{\text{obs}}| - |F_{\text{calc}}|) / \sum_{\text{ref}} |F_{\text{obs}}|$.

TABLE II. Atomic coordinates and isotropic temperature factors for $R_2\text{BaNiO}_5$, with standard deviations in parentheses.

Atom	x/a	y/b	z/c	U_{eq}^a
Y	0	0	0.2027(1)	1.8(3)
Ba	0	0.5	0	5.1(3)
Ni	0.5	0	0	2.7(5)
O(1)	0.5	0.2408(8)	0.1487(3)	5(1)
O(2)	0	0	0	4(2)
Er	0	0	0.2031(1)	3(1)
Ba	0	0.5	0	7(1)
Ni	0.5	0	0	6(1)
O(1)	0.5	0.2385(29)	0.1507(13)	14(4)
O(2)	0	0	0	13(9)

$$^a U_{\text{eq}} = \frac{1}{3} \sum_{i,j} [U_{ij} a_i^* a_j^* a_i a_j \cos(a_i, a_j)] \times 10^{-3}.$$

RESULTS AND DISCUSSION

Crystal structure

Atomic coordinates for $R_2\text{BaNiO}_5$ ($R = \text{Y, Er}$) are shown in Table II. Table III includes bond lengths and angles. For $R = \text{Er}$ all the dimensions are very similar to those of the Y compound. There are three slightly different $R\text{-O}$ distances, as Table III shows. RO_7 polyhedra share different elements in each direction of the space giving rise to two kinds of interstices. Those in the a direction (Fig. 1) show the form of flattened octahedra with four equal $\text{NiO}(1)$ equatorial distances and two $\text{NiO}(2)$ apical, 0.3 \AA shorter. The NiO_6 flattened octahedra share $\text{O}(2)$ vertices with each other, being the Ni-O-Ni distances 3.76 and 3.75 \AA , respectively, even shorter than in the Gd compound.¹² The interstices formed in the b direction are bicapped quadrangular cavities which house the Ba^{2+} cations. These three kinds of polyhedra converge at the $\text{O}(2)$ atoms, and the structure consists of blocks of RO_7 polyhedra sharing two edges of their largest quadrangular faces, in the a direction. Two of these blocks are opposite each other in the c direction, as Fig. 2

TABLE III. Bond distances (\AA) and angles ($^\circ$) and principal interatomic distances in BaR_2NiO_5 .

			$R = \text{Er}$	$R = \text{Y}$
Ba	O(1)	[8]	2.941(12)	2.933(3)
	O(2)	[2]	2.869(1)	2.8805(3)
R	O(1)	[4]	2.394(10)	2.416(3)
	O(1)	[2]	2.229(15)	2.250(4)
	O(2)	[1]	2.292(1)	2.2952(8)
Ni	O(1)	[4]	2.183(15)	2.182(4)
	O(2)	[2]	1.874(1)	1.8805(3)
R	R	[4]	3.586(1)	3.6029(4)
		[2]	3.747(2)	3.7610(6)
Ni	Ni	[2]	3.747(2)	3.7610(6)
O(1)-Ni-O(1)		[2]	180.0(3)	180.0(5)
		[2]	102.3(6)	101.0(2)
		[2]	77.7(6)	79.0(2)
		[8]	90.000(1)	90.000(2)
O(2)-Ni-O(2)	[1]	180	180	

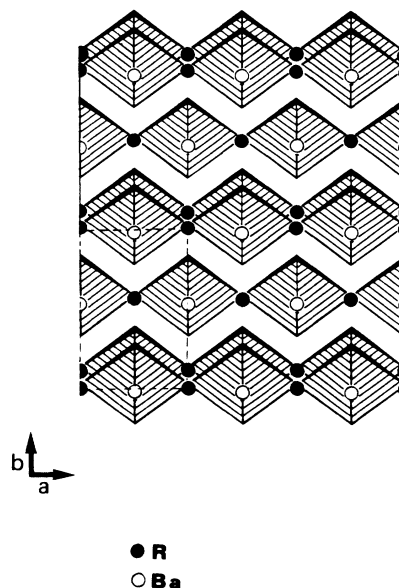


FIG. 1. View along the c direction (rotated 10°) showing the chains of NiO_6 octahedra.

shows, and share the vertex occupied by the $\text{O}(2)$ atom. The set formed by two blocks is joined along the b direction to the other two sets, one placed above it and the other below. This second set is also shown in Fig. 2.

Magnetic measurements

Tables IV and V show the x-ray diffraction data for polycrystalline samples of the Y and Er compounds, re-

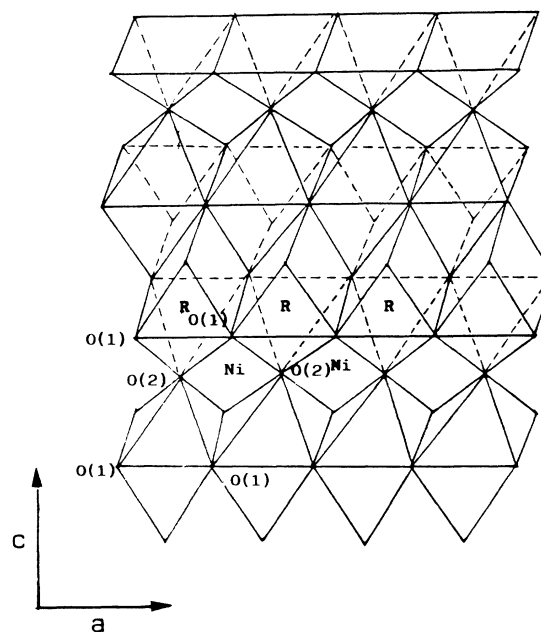


FIG. 2. Perspective of the packing of RO_7 polyhedra in the crystal structure of $R_2\text{BaNiO}_5$.

spectively. The temperature dependence of the magnetic susceptibility for Y_2BaNiO_5 is shown in Fig. 3. A progressive decreasing in the susceptibility can be observed with decreasing temperatures until 60 K. Below this temperature the susceptibility remains almost constant until 20 K. At the lowest temperatures down to 4.2 K a sharp field dependence increasing is observed. The susceptibility at room temperature is 1.093×10^{-3} emu mol $^{-1}$, a value rather smaller than that expected for Ni^{2+} with two unpaired localized electrons and $S=1$. This behavior can be attributed to the superexchange interactions due to the strong O- e_g -O overlapping at 180° of

the oxygen p orbitals and the Ni^{2+} d orbitals giving rise to strong antiferromagnetic interactions. These interactions are more intense than those present in La_2NiO_4 , although Ni^{2+} ions have two magnetic neighbors in linear Y_2BaNiO_5 and four in layered La_2NiO_4 . The shorter Ni-O-Ni distances in Y_2BaNiO_5 , 3.76 Å, as compared with those¹⁹ in La_2NiO_4 , 3.86 Å, justify for the Y oxide a more effective O- e_g -O overlapping, stronger superexchange interactions, and the ordering of the Ni^{2+} ions along the chains of NiO_6 flattened octahedra at room temperature. The increase of susceptibility observed below 20 K could be due to two possible causes. At these low temperatures

TABLE IV. X-ray diffraction data for polycrystalline Y_2BaNiO_5 .

h	k	l	d_{obs}	d_{calc}	I_{obs}	I_{calc}	h	k	l	d_{obs}	d_{calc}	I_{obs}	I_{calc}	
0	0	2	5.68	5.67	18	22	3	2	1	1.1434	1.1434	>	43	16
0	1	1	5.15	5.14	13	8	2	4	0		1.1433	>		46
1	0	1	3.572	3.568	93	98	0	0	10	1.1332	1.1332		12	14
0	1	3	3.160	3.159	277	283	1	2	9		1.1029	>		12
0	2	0	2.881	2.880	279	279	0	5	3	1.1018	1.1021	>	19	12
0	0	4	2.834	2.833	113	122	3	0	5	1.0969	1.0968		18	18
1	1	2	2.753	2.752	1000	1000	1	3	8	1.0909	1.0909		32	41
1	0	3	2.653	2.665	12	2	1	5	2	1.0814	1.0814		39	46
0	2	2	2.5686	2.5677	25	22	2	4	4	1.0603	1.0602		19	21
1	2	1		2.2415		175	0	2	10	1.0546	1.0545		31	36
0	1	5		2.1090	>		2	3	7	1.0338	1.0338		24	24
1	1	4	2.1072	2.1060	>	72	3	3	2	1.0320	1.0320		35	42
0	2	4	2.0198	2.0198	189	199	3	1	6	1.0280	1.0276		12	7
1	2	3	1.9564	1.9561	45	42	3	2	5	1.0249	1.0250		24	29
1	0	5	1.9416	1.9411	126	128	2	4	6	0.9783	0.9781		19	24
0	0	6	1.8891	1.8886	66	61	2	0	10	0.9706	0.9705		15	20
2	0	0	1.8804	1.8801	141	148	0	6	0	0.9600	0.9602		12	10
0	3	3	1.7118	1.7118	43	41	2	5	3	0.9507	0.9508		15	20
1	3	2	1.6371	1.6372	180	198	4	0	0	0.9400	0.9400		15	15
1	1	6	1.6199	1.6196	42	34	0	5	7	0.9389	0.9387		16	10
2	1	3	1.6156	1.6156	93	77	1	6	1		0.9271			11
1	2	5	1.6097	1.6097	137	124	3	1	8	0.9266	0.9264		27	33
0	2	6		1.5794		32	2	2	10	0.9196	0.9197		42	60
2	2	0	1.5749	1.5744	96	86	1	4	9		0.9192			14
2	0	4	1.5667	1.5665	46	39	0	6	4		0.9094			15
0	1	7	1.5584	1.5585	40	38	1	1	12	0.9046	0.9045		28	41
1	0	7	1.4882	1.4869	13	10	4	1	3	0.9011	0.9010		17	18
0	3	5		1.4651	>		4	2	0	0.8937	0.8937		17	20
1	3	4	1.4644	1.4641	>	22	0	4	10	0.8906	0.8906		17	20
0	4	0	1.4409	1.4402	56	54	3	4	5	0.8725	0.8726		19	31
2	1	5	1.4037	1.4034	18	15	1	5	8	0.8696	0.8696		23	36
2	2	4	1.3760	1.3762	73	94	1	6	5	0.8605	0.8606		19	31
1	4	1	1.3355	1.3359	16	12	4	1	5	0.8586	0.8586		14	5
2	0	6	1.3325	1.3324	35	32	2	6	0		0.8551			23
1	1	8		1.2918		73	4	2	4	0.8523	0.8523		21	34
0	4	4	1.2839	1.2839	24	19	3	2	9		0.8488			12
2	3	3	1.2657	1.2657	26	30	3	3	8	0.8435	0.8433			38
0	3	7	1.2377	1.2377	16	19	2	5	7	0.8394	0.8398		23	23
2	2	6	1.2093	1.2093	14	24	3	5	2	0.8390	0.8388		25	44
2	1	7	1.1998	1.1998	30	31	1	3	12	0.8266	0.8267		23	53
3	1	2	1.1971	1.1971	59	63	4	3	3		0.8240			23
1	0	9		1.1939		12	2	6	4	0.8186	0.8186		16	40
1	4	5	1.1565	1.1566	37	42	4	1	7		0.8049			34
0	4	6	1.1452	1.1452	21	18	2	4	10	0.8049	0.8048		34	62
							1	7	2	0.7959	0.7960		25	69

it is possible that some interchain ferromagnetic interactions could be operative, giving rise to a tridimensional magnetic order; however, the presence and/or some ferromagnetic impurities cannot be discarded.

The reciprocal susceptibility for $\text{Er}_2\text{BaNiO}_5$ is displayed in Fig. 4. In the 300–40 K temperature range a Curie-Weiss behavior can be observed, since $\chi = 11.50/(T + 0.94)$. Below 40 K the experimental data exhibit a strong deviation from the Curie-Weiss law and the curve bends upward showing a minimum at 15 K. The magnetic moment calculated from the Curie-Weiss law is $9.59\mu_B$ which fairly agrees with that expected,

$9.6\mu_B$, for the free Er^{3+} ion.²⁰ The contribution to the susceptibility of Ni^{2+} , expected to be antiferromagnetically ordered as in isostructural Y_2BaNiO_5 , should be very small and will be masked by the strong paramagnetic signal due to the f electrons of the Er^{3+} ions. The low-temperature data are better illustrated in the χ versus T plot, as shown in the inset in Fig. 4. The maximum observed in χ at 15.6 K can be attributed to tridimensional antiferromagnetic ordering of the Er^{3+} ions. Below this temperature the susceptibility sharply falls in such a way that the magnetic moment of Er^{3+} at the liquid helium temperature only reaches about $3\mu_B$. This is unusual and

TABLE V. X-ray diffraction data for polycrystalline $\text{Er}_2\text{BaNiO}_5$.

<i>h</i>	<i>k</i>	<i>l</i>	d_{obs}	d_{calc}	I_{obs}	I_{calc}	<i>h</i>	<i>k</i>	<i>l</i>	d_{obs}	d_{calc}	I_{obs}	I_{calc}
0	0	2	5.68	5.65	19	20	3	2	1		1.1406		14
0	1	1	5.19	5.11	19	20	2	4	0	1.1399	1.1393	47	44
1	0	1	3.571	3.561	103	102	0	0	10	1.1292	1.1293	13	15
0	1	3	3.177	3.147	356	344	1	2	9		1.0991	>	13
0	2	0	2.874	2.868	304	304	0	5	3	1.0977	1.0974	>	14
0	0	4	2.829	2.823	123	105	3	0	5	1.0945	1.0942		26
1	1	2	2.749	2.744	1000	1000	1	3	8	1.0870	1.0870	32	40
1	0	3	2.663	2.658	19	14	1	5	2	1.0772	1.0769	38	46
1	2	1		2.2336		148	2	4	4	1.0565	1.0562	14	18
0	1	5	2.1028	2.1016	80	72	0	2	10	1.0508	1.0508	26	35
1	1	4		2.0995		10	1	4	7		1.0306	>	10
0	2	4	2.0115	2.0120	162	155	2	3	7	1.0304	1.0303	>	36
1	2	3	1.9512	1.9493	85	80	3	3	2	1.0295	1.0292	40	42
1	0	5	1.9362	1.9351	157	153	3	2	5	1.0224	1.0223	29	35
0	0	6	1.8828	1.8822	62	44	2	4	6	0.9749	0.9747	15	18
2	0	0	1.8775	1.8761	140	141	2	0	10	0.9678	0.9676	16	21
0	3	3	1.7050	1.7047	>	65	0	6	0	0.9564	0.9560	9	11
1	3	0		1.7036	>	11	2	5	3	0.9477	0.9473	17	22
1	3	2	1.6315	1.6310	188	198	4	0	0		0.9381	>	15
1	1	6		1.6144		15	0	5	7	0.9352	0.9349	>	20
2	1	3	1.6115	1.6115	96	94	3	1	8	0.9240	0.9239	30	32
1	2	5	1.6047	1.6041	161	151	1	6	1		0.9233		10
0	2	6		1.5736		24	2	2	10	0.9168	0.9168	47	58
2	2	0	1.5709	1.5701	92	95	1	4	9		0.9158		14
2	0	4	1.5633	1.5626		34	0	6	4	0.9059	0.9055	11	12
0	1	7	1.5531	1.5531	52	48	1	1	12	0.9014	0.9015	>	59
1	0	7	1.4822	1.4821	20	19	4	1	3	0.8992	0.8990	>	22
0	3	5	1.4596	1.4593	22	20	4	2	0	0.8919	0.8916	16	22
0	4	0	1.4348	1.4340	51	52	0	4	10	0.8875	0.8872	18	22
2	1	5	1.3998	1.3996	35	33	3	4	5	0.8699	0.8701	18	37
2	2	4	1.3723	1.3721	61	74	1	5	8	0.8667	0.8662	23	35
1	4	1	1.3310	1.3302	19	12	1	6	5	0.8574	0.8571	26	37
2	0	6	1.3289	1.3287	29	23	4	1	5		0.8566		11
1	1	8	1.2877	1.2875		71	2	6	0	0.8525	0.8518	18	24
0	4	4	1.2791	1.2785	17	17	4	2	4	0.8503	0.8502	25	27
2	3	3	1.2617	1.2620	39	34	3	2	9		0.8464		12
0	3	7	1.2333	1.2330	19	23	3	3	8	0.8410	0.8408	25	37
3	1	0	1.2100	1.2220	8	3	2	5	7	0.8368	0.8368	31	30
2	2	6	1.2059	1.2057	22	19	3	5	2		0.8361		45
2	1	7	1.1965	1.1964	44	40	1	3	12	0.8238	0.8238	30	55
3	1	2	1.1946	1.1944	57	63	2	6	4	0.8158	0.8155	18	33
1	0	9		1.1900		11	4	1	7		0.8029		41
1	4	5	1.1524	1.1521	>	54	2	4	10	0.8022	0.8021	32	69
2	3	5		1.1519	>	15	1	7	2	0.7929	0.7926	27	73
0	4	6		1.1407		13							

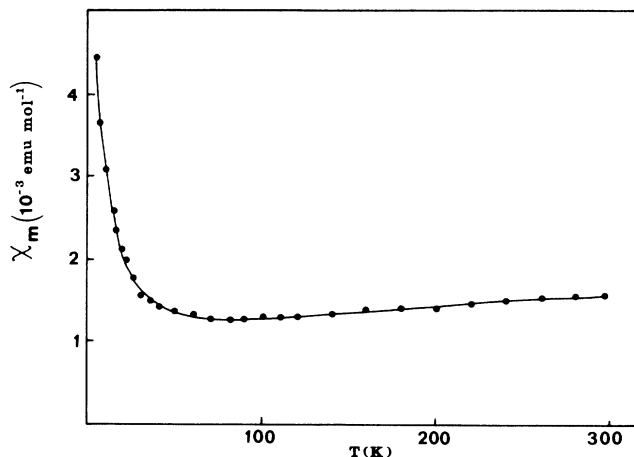


FIG. 3. Temperature dependence of the magnetic susceptibility per mole of Ni^{2+} of Y_2BaNiO_5 .

indicates strong interactions which mask the expected crystal-field effect ordinarily present in the Er mixed oxides at this lower temperature.^{21,22} Although antiferromagnetic order has been recently reported in some $R_2\text{MO}_4$ oxides, R being a rare earth and M equal to Ni or Cu, in all cases the Néel temperatures are^{23,24} below 15.6 K.

In summary, the oxides formulated $R_2\text{BaNiO}_5$ ($R = \text{Y}, \text{Er}$) exhibit very interesting structural and magnetic properties. In the Y compound, chains of NiO_6 flattened octahedra and extremely short Ni-O-Ni distances explain the behavior of Ni^{2+} ions as a monodimensional 1D system, in which they become antiferromagnetically ordered below 300 K. Moreover, in the Y oxide some ferromagnetic interactions are operative below 40 K as a consequence of tridimensional interchain interactions and/or the presence of ferromagnetic impurities. The estimated Néel temperature for this oxide is comparatively higher than the value of 28 K reported⁶ from neutron diffraction data for the analogous Y_2BaCuO_5 . The mentioned structural differences between both compounds should be responsible for such distinct behavior. Whereas in Y_2BaNiO_5 the superexchange Ni-O-Ni is clearly promoted along the chains of sharing-corners flattened NiO_6 octahedra, the low Néel temperature of 28 K for Y_2BaCuO_5 is due to the absence of a direct network

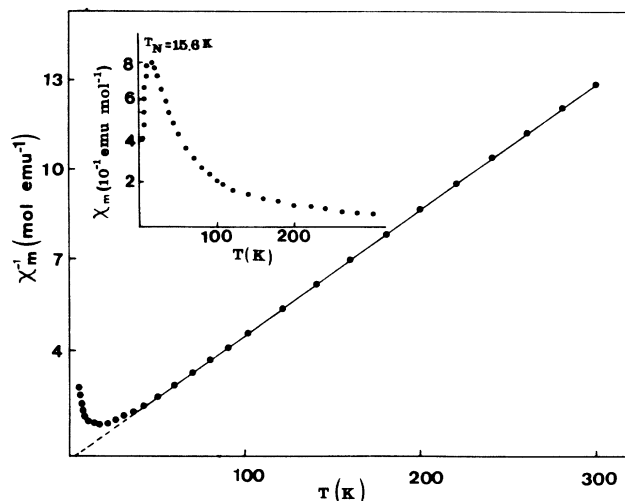


FIG. 4. Temperature variation of the reciprocal magnetic susceptibility per mole of Er^{3+} in $\text{Er}_2\text{BaNiO}_5$. In the inset, plotting of the magnetic susceptibility per mole of Er^{3+} in $\text{Er}_2\text{BaNiO}_5$, as a function of the temperature.

Cu-O-Cu superexchange path in its structure. In the case of the Er oxide, both effects are masked by the strong paramagnetic signal of Er^{3+} , and the maximum observed for the susceptibility at 15.6 K can be attributed to a tridimensional ordering of the Er^{3+} ions.

Although the key factor of the interesting properties exhibited by the $R_2\text{BaNiO}_5$ oxides appears to be the presence of chains of flattened NiO_6 octahedra with short Ni-O-Ni distances, we have grown crystals of the Nd, Sm, Eu, Dy, and Ho compounds and we are performing magnetic measurements on polycrystalline samples of these oxides to further elucidate the nature of the antiferromagnetic order which they exhibit. We are also currently undertaking neutron diffraction measurements to explore their magnetic structure. Listings of anisotropic thermal parameters for Y_2BaNiO_5 and $\text{Er}_2\text{BaNiO}_5$ and of observed and calculated structure factors are available.²⁵

ACKNOWLEDGMENTS

The authors are indebted to the Spanish Comisión Interministerial de Ciencia y Tecnología for financial support under Project No. MAT 88-0250-C 02.

*Also at the Grupo de Difracción, Facultad de Ciencias Químicas, Universidad Complutense, 28040 Madrid, Spain.

†Author to whom correspondence should be addressed.

¹C. Michel and B. Raveau, *J. Solid State Chem.* **43**, 73 (1982).

²C. Michel and B. Raveau, *J. Solid State Chem.* **49**, 150 (1983).

³S. Schiffler and H. Müller-Buschbaum, *Z. Anorg. Allg. Chem.* **540-541**, 243 (1986).

⁴J. A. Campá, J. M. Gómez de Salazar, E. Gutiérrez Puebla, M. A. Monge, I. Rasines, and C. Ruiz-Valero, *Phys. Rev. B* **37**, 529 (1988).

⁵M. Taïbi, J. Aride, E. Antic-Fidancev, M. Lemaitre-Blaise, P. Porcher, and P. Caro, *J. Solid State Chem.* **74**, 329 (1988).

⁶T. Chattopadhyay, P. J. Brown, U. Köbler, and M. Wilhelm, *Europhys. Lett.* **8**, 685 (1989).

⁷S. Schiffler and H. Müller-Buschbaum, *Z. Anorg. Allg. Chem.* **532**, 10 (1986).

⁸S. Schiffler and H. Müller-Buschbaum, *Monatsh. Chem.* **118**, 741 (1987).

⁹H. Müller-Buschbaum and C. Lang, *J. Less-Common Met.* **142**, L1 (1988).

- ¹⁰H. Müller-Buschbaum and I. Rüter, *Z. Anorg. Allg. Chem.* **572**, 181 (1989).
- ¹¹J. Amador, Doctoral thesis, Universidad Autónoma de Madrid, 1989.
- ¹²J. Amador, E. Gutiérrez Puebla, M. A. Monge, I. Rasines, J. A. Campá, J. M. Gómez de Salazar, and C. Ruiz Valero, *Solid State Ion.* **32-33**, 123 (1989).
- ¹³J. K. Burdett and J. F. Mitchell, *J. Am. Chem. Soc.* **112**, 6571 (1990).
- ¹⁴*International Tables for X-ray Crystallography*, edited by C. H. Macgillavry and G. D. Rieck (Kynoch, Birmingham, England, 1983), Vol. III, pp. 210–216.
- ¹⁵N. Walker and S. Stuart, *Acta Crystallogr. Sect. A* **39**, 158 (1983).
- ¹⁶J. M. Stewart, F. A. Kundell, and J. C. Baldwin, *The X-ray 80 System* (Computer Science Center, University of Maryland, College Park, Maryland, 1980).
- ¹⁷F. Fernández, R. Sáez-Puche, C. Cascales, C. M. Marcano, and I. Rasines, *J. Phys. Chem. Solids* **50**, 871 (1989).
- ¹⁸*Theory and Applications of Molecular Paramagnetism*, edited by E. A. Boudreaux and L. N. Mulay (Wiley, New York, 1976), p. 494.
- ¹⁹J. B. Goodenough and A. Ramasesha, *Mater. Res. Bull.* **17**, 383 (1982).
- ²⁰Boudreaux and Mulay (Ref. 18), p. 307.
- ²¹M. D. Guo, A. T. Aldred, and S. K. Chan, *J. Phys. Chem. Solids* **48**, 229 (1987).
- ²²Y. Laureino, A. Jerez, F. Fernández, R. Sáez-Puche, M. L. Veiga, and C. Pico, *J. Less-Common Met.* **157**, 335 (1990).
- ²³J. Rodríguez-Carvajal, M. T. Fernández, J. L. Martínez, F. Fernández, and R. Sáez-Puche, *Europhys. Lett.* **11**, 261 (1990).
- ²⁴R. Sáez-Puche, M. Norton, T. R. White, and W. S. Glaunsinger, *J. Solid State Chem.* **50**, 281 (1983).
- ²⁵See AIP document No. PAPS-PRBMD-42-7918-06 for listings of anisotropic thermal parameters for Y_2BaNiO_5 (1 page) and $\text{Er}_2\text{BaNiO}_5$ (1 page); and listings of observed and calculated structure factors for Y_2BaNiO_5 (2 pages) and $\text{Er}_2\text{BaNiO}_5$ (2 pages). Order by PAPS number and journal reference from American Institute of Physics, Auxiliary Publication Service, 335 East 45th Street, New York, NY 10017. The prices are \$1.50 for microfiche and \$5 for photocopies. Airmail additional. Make checks payable to the American Institute of Physics.